Cell PRESS
Neuron
Article

Drosophila Pacemaker Neurons Require G Protein Signaling and GABAergic Inputs to Generate Twenty-Four Hour Behavioral Rhythms

David Dahdal,[1] David C. Reeves,[2,3] Marc Ruben,[1] Myles H. Akabas,[2] and Justin Blau[1,*]
[1]Department of Biology, New York University, 100 Washington Square East, New York, NY 10003, USA
[2]Department of Physiology and Biophysics and Department of Neuroscience, Albert Einstein College of Medicine of Yeshiva University, Bronx, NY 10461, USA
[3]Present address: ARMGO Pharma Inc., 777 Old Saw Mill River Road, Tarrytown, NY 10591, USA
*Correspondence: justin.blau@nyu.edu
DOI 10.1016/j.neuron.2010.11.017

SUMMARY

Intercellular signaling is important for accurate circadian rhythms. In *Drosophila*, the small ventral lateral neurons (s-LN$_v$s) are the dominant pacemaker neurons and set the pace of most other clock neurons in constant darkness. Here we show that two distinct G protein signaling pathways are required in LN$_v$s for 24 hr rhythms. Reducing signaling in LN$_v$s via the G alpha subunit Gs, which signals via cAMP, or via the G alpha subunit Go, which we show signals via Phospholipase 21c, lengthens the period of behavioral rhythms. In contrast, constitutive Gs or Go signaling makes most flies arrhythmic. Using dissociated LN$_v$s in culture, we found that Go and the metabotropic GABA$_B$-R3 receptor are required for the inhibitory effects of GABA on LN$_v$s and that reduced GABA$_B$-R3 expression in vivo lengthens period. Although no clock neurons produce GABA, hyperexciting GABAergic neurons disrupts behavioral rhythms and s-LN$_v$ molecular clocks. Therefore, s-LN$_v$s require GABAergic inputs for 24 hr rhythms.

INTRODUCTION

Circadian rhythms are found in organisms as diverse as plants and humans. In all organisms so far studied, these ~24 hr rhythms are driven by intracellular molecular clocks that consist of transcriptional/translational feedback loops with additional posttranslational regulation. The importance of molecular clocks in determining period length is exemplified by the numerous clock gene mutations that alter molecular clock speed and behavioral rhythms (reviewed by Allada et al., 2001). Since many mammalian cells show rhythmic clock gene expression in culture, intracellular clocks are often considered cell-autonomous (Balsalobre et al., 1998; Welsh et al., 1995).

However, intercellular communication is also important for circadian rhythms. For example, signals from master pacemaker neurons in the mammalian suprachiasmatic nucleus (SCN) regulate the phase of clocks in peripheral organs (Reppert and Weaver, 2002). Coupling of pacemaker neurons within the SCN is also important because individual pacemaker neurons from a single animal display a range of periods of electrical rhythms when dispersed in culture, whereas only one period is measured in SCN explants and animals (Herzog et al., 1998; Liu et al., 1997). Similarly, deletions of either *mPeriod1* (*mPer1*) or *mCryptochrome1* (*mCry1*) clock genes dramatically weakened molecular rhythms in individual dissociated SCN cells but had minimal effects on molecular rhythms in SCN explants or animal behavioral rhythms (Liu et al., 2007). Presumably, coupling between cells rescues the genetically weakened individual SCN oscillators and suggests that signaling between clock neurons is essential for robust SCN rhythms.

Further support for SCN intercellular communication comes from *VPAC$_2$R$^{-/-}$* mice. VPAC$_2$R encodes a G protein coupled receptor (GPCR) expressed by many SCN neurons and is activated by the neuropeptides VIP and PACAP (Harmar et al., 1998). *VPAC$_2$R$^{-/-}$* mutant mice are behaviorally arrhythmic (Harmar et al., 2002), and most neurons in SCN slices from *VPAC$_2$R$^{-/-}$* mutants lose *mPer1::luciferase* rhythms (Maywood et al., 2006). Thus, disrupting a membrane-bound receptor that presumably acts as an input to SCN neurons prevented molecular rhythms even though core clock genes were genetically unaffected.

Drosophila have ~150 clock neurons in discrete clusters in the brain, named after their location: In each hemisphere, there are four small and four large ventral lateral neurons (s- and l-LN$_v$s) that synthesize the key circadian neuropeptide Pigment-Dispersing Factor (PDF). There are also a fifth PDF-negative s-LN$_v$, six dorsal lateral neurons (LN$_d$s), three lateral posterior clock neurons (LPNs), and ~50 clock neurons located in three different dorsal clusters (DN$_{1-3}$). Overexpression of the Shaggy/GSK3 (Sgg) kinase only in s-LN$_v$s speeds up their own molecular clocks and the clocks in most other central brain clock neurons. In contrast, *sgg* overexpression in all clock neurons except LN$_v$s does not alter the speed of s-LN$_v$ or most other molecular clocks (Stoleru et al., 2005). Therefore, s-LN$_v$s seem to be the master pacemakers in constant darkness (DD) and set the pace for much of the *Drosophila* clock network. Although the ability of individual *Drosophila* clock neurons to generate 24 hr rhythms has not been tested in culture, intercellular

communication between *Drosophila* pacemaker neurons could explain how molecular and behavioral rhythms persist in DD in vivo (Lin et al., 2004; Peng et al., 2003; Yoshii et al., 2009). In contrast, oscillations in peripheral clocks, which are not coupled to each other, dampen in DD (Stanewsky et al., 1997).

Although s-LN_vs are pacemakers in DD, they require signals from their cell membrane for 24 hr rhythms. For example, s-LN_v molecular clocks desynchronize and/or run down in DD in Pdf^{01} null mutant flies (Lin et al., 2004; Peng et al., 2003; Yoshii et al., 2009) and run down when hyperpolarized in DD (Nitabach et al., 2002). Pdf^{01} and *PDF receptor* (*pdfr*) mutant flies are either arrhythmic or have short period behavioral rhythms in DD (Hyun et al., 2005; Lear et al., 2005; Mertens et al., 2005; Renn et al., 1999). Like $VPAC_2R$, the PDFR is a GPCR that signals via cAMP at least in vitro (Hyun et al., 2005; Mertens et al., 2005), and LN_vs also seem to respond to PDF (Im and Taghert, 2010; Shafer et al., 2008).

LN_vs also respond to neurotransmitters from other neurons. The Hofbauer-Buchner eyelet photoreceptor cells project to LN_vs and produce acetylcholine (ACh) and histamine (Pollack and Hofbauer, 1991; Yasuyama and Meinertzhagen, 1999). Serotonergic neurons project to adult LN_vs and modulate light entrainment via the metabotropic 5-HT1B receptor in LN_vs (Yuan et al., 2005), and l-LN_vs respond to GABA via the ionotropic $GABA_A$ receptor, RDL, to regulate sleep and arousal (Chung et al., 2009; Parisky et al., 2008). Larval LN_vs, which become the adult s-LN_vs, respond directly to ACh, GABA, and glutamate in vitro and produce glutamate and GABA metabotropic receptors (Hamasaka et al., 2007; Hamasaka et al., 2005; Wegener et al., 2004). Although glutamatergic and GABAergic neurons project to larval and adult LN_vs (Hamasaka et al., 2007; Hamasaka et al., 2005), their role in circadian rhythms is largely unknown.

We first addressed the role of GPCRs in s-LN_vs by manipulating G protein signaling. We focused on two G protein alpha subunits: G-sα60A (Gs), which activates Adenylate cyclase to produce cAMP, and G-oα47A (Go), whose signaling mechanism was unclear previous to this study but probably is cAMP independent (Ferris et al., 2006). We found that reduced signaling via either Gs or Go in LN_vs lengthened the period of behavioral rhythms, while constitutively activating Gs or Go made flies largely arrhythmic. In epistasis experiments, expressing the cAMP phosphodiesterase *dunce* (*dnc)* rescued the arrhythmicity of constitutively active Gs and lengthened period when expressed alone, showing that Gs signals via cAMP to regulate period length in LN_vs. Similarly, reducing *Phospholipase C 21C* (*Plc21C*) expression rescued arrhythmicity induced by a constitutively active Go transgene and lengthened behavioral period on its own, indicating that PLC21C lies downstream of Go in LN_vs. Given this previously unsuspected role of Go signaling in maintaining 24 hr rhythms in LN_vs, we sought to identify potential receptors and ligands that signal via Go.

We measured Ca^{2+} responses of dissociated LN_vs in culture and found that inhibiting Go made LN_vs unresponsive to GABA but did not affect LN_v responses to ACh or glutamate. We found that GABA probably signals via the metabotropic GABA receptor $GABA_B$-*R3* in LN_vs since knocking down its expression strongly reduced the response to GABA in culture and lengthened behavioral rhythms in adult flies. Although LN_vs do not produce GABA themselves (Hamasaka et al., 2005), we found that hyperexciting GABAergic neurons disrupts animal behavioral rhythms and s-LN_v molecular clocks. Therefore, s-LN_vs integrate signals from GABAergic neurons as part of a network that generates 24 hr rhythms.

RESULTS

Gs-Mediated Signaling in LN_vs Is Required for 24 Hr Rhythms

The neuropeptide PDF is the only described signal that s-LN_vs require to maintain synchronous molecular oscillations (Lin et al., 2004; Peng et al., 2003). s-LN_vs probably use PDF to signal to each other since they express PDFR (Im and Taghert, 2010), a GPCR that probably couples to Gs (Hyun et al., 2005; Mertens et al., 2005; Shafer et al., 2008). To test how important Gs signaling in LN_vs is for circadian rhythms, we assayed the behavior of flies with altered *Gs* expression or activity in LN_vs.

We first measured the locomotor activity in DD of flies in which *Gs* RNA levels were reduced specifically in LN_vs using two copies of the *Pdf-Gal4* driver to express a previously described *UAS-Gs-RNAi* transgene (Ueno et al., 2006). The average period of these *Pdf > Gs-RNAi* flies was 25.0 hr, significantly longer than the 24.0 or 23.8 hr periods of control flies with *Pdf-Gal4* or *UAS-Gs-RNAi* alone ($p < 0.001$) (Figure 1A and Table1). Next we assayed flies expressing either wild-type Gs or Gs carrying a point mutation that eliminates its intrinsic GTPase activity and makes Gs constitutively active (*UAS-Gs* and *UAS-Gs-GTP* respectively, (Wolfgang et al., 1996). We found that more than 60% of *Pdf > Gs* and *Pdf > Gs-GTP* flies were arrhythmic, whereas the rhythmic flies had normal periods but were only weakly rhythmic, as shown by a lower rhythm power than control flies (Figure 1A and Table1). We checked for the presence of s-LN_vs in *Pdf > Gs-GTP* flies, using antibodies to PDF and found that s-LN_vs project normally to the dorsal brain and also express the clock proteins Vrille (VRI) and PER at ZT20 (ZT: Zeitgeber time, time in a 12:12 LD cycle) (see Figure S1 available online). Therefore, the arrhythmicity of many *Pdf > Gs-GTP* flies is not due to loss of s-LN_vs or to visible developmental defects.

cAMP phosphodiesterases, such as DNC, reduce Gs-mediated signaling by hydrolyzing cAMP to AMP. Therefore, we used a *UAS-dnc* transgene (Cheung et al., 1999) to decrease cAMP levels as an independent way to alter Gs signaling activity in LN_vs. We found that *Pdf > dnc* flies had much longer periods than control *UAS-dnc* flies (26.6 hr versus 24.0 hr, respectively, $p < 0.001$) (Figure 1B and Table 1). We also found that the arrhythmicity caused by expressing Gs-GTP in LN_vs could be completely rescued by coexpression of *UAS-dnc* but not by coexpressing a control transgene, *UAS-CD8::GFP* (Figure 1C and Table 1). Thus, the effects of Gs on circadian rhythms are mediated via cAMP rather than direct effects of activated Gs on ion channels. We also noticed that *Pdf > Gs-GTP + dnc* flies have ~2 hr shorter periods than *Pdf > dnc* flies, suggesting that cAMP levels help determine period length as in mammals (O'Neill et al., 2008). Similarly, flies with only one copy of *Pdf-Gal4* expressing *UAS-dnc* have shorter periods (25.5 hr)

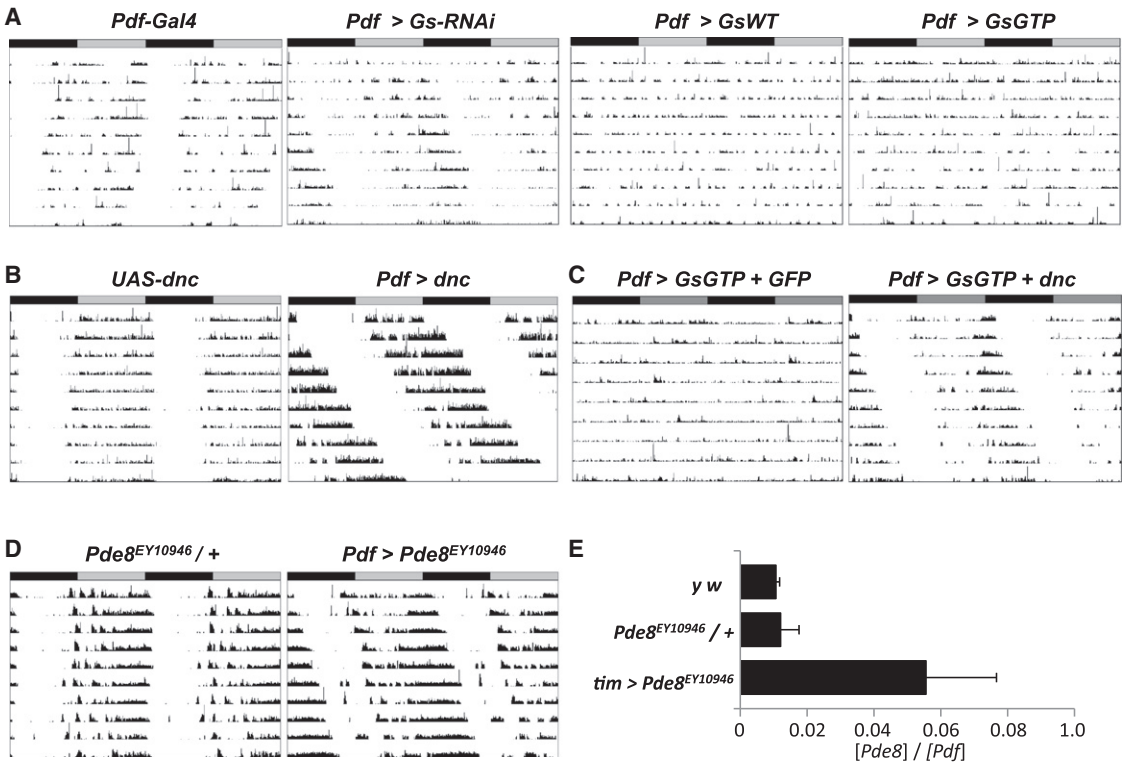

Figure 1. Normal Gs Signaling in LN_vs Is Required for 24 Hour Locomotor Rhythms

(A–D) Representative actograms showing locomotor activity in DD of flies with manipulations to Gs signaling in LN_vs. Actograms are double-plotted with gray and black bars indicating prior LD cycles.

(A) Left: Control fly homozygous for two *Pdf-Gal4* transgenes with 24.0 hr period. The next three panels (from left to right) show activity of flies with *Pdf-Gal4* expressing transgenes with RNAi directed against *Gs* (*Pdf* > *Gs-RNAi*), wild-type *Gs* (*Pdf* > *Gs*), or constitutively active *Gs* (*Pdf* > *Gs-GTP*). *Pdf* > *Gs-RNAi* flies had longer period rhythms (25.0 hr) than controls ($p < 0.0001$ versus *Pdf-Gal4* and *UAS-Gs-RNAi* / + flies). *Pdf* > *Gs* and *Pdf* > *Gs-GTP* flies were either arrhythmic or had weaker rhythms than controls.

(B) Left: fly with a *UAS-dnc* transgene (*UAS-dnc*, 24.0 hr). Right: fly with *UAS-dnc* expressed in LN_vs (*Pdf* > *dnc*, 26.6hr). *Pdf* > *dnc* flies have longer periods than controls ($p < 0.001$).

(C) Flies with *Pdf-Gal4* expressing *UAS-Gs-GTP* and either a *UAS-CD8::GFP* transgene (*Pdf* > *GsGTP* + *GFP*, left) or a *UAS-dnc* transgene (*Pdf* > *GsGTP* + *dnc*, right).

(D) Left: Fly heterozygous for a P-element in *Pde8* (*Pde8*^{EY10946} / +, 24.2 hr). Right: Fly with *Pde8* misexpressed in LN_vs (*Pdf* > *Pde8*^{EY10946}, 25.0 hr, right). *Pdf* > *Pde8*^{EY10946} flies have longer periods than controls ($p < 0.001$).

(E) RNA was isolated from heads of *y w* and *Pde8*^{EY10946} / + control flies and from flies with *tim(UAS)-Gal4* misexpressing *Pde8*^{EY10946} (*tim* > *Pde8*^{EY10946}). Levels of *Pde8* and *Pdf* RNA were measured by qPCR, and the relative level (*Pde8*: *Pdf*) was plotted, with error bars showing SEM. Since *tim* > *Pde8*^{EY10946} flies have more *Pde8* RNA than controls ($p < 0.01$), Gal4-activated *Pde8*^{EY10946} misexpresses *Pde8*.

than flies with two copies of *Pdf-Gal4* (26.6 hr): presumably, the latter have higher DNC levels and lower cAMP levels.

We also tested whether period length could be altered by misexpressing PDE8, another cAMP-specific phosphodiesterase (Day et al., 2005). We found that *Pdf* > *Pde8*^{EY10946} flies have longer period rhythms than control flies (25.0 hr) (Figure 1D and Table 1). We confirmed that this previously uncharacterized *Pde8* P-element insertion that contains binding sites for Gal4 increases *Pde8* RNA levels when activated by a Gal4 driver (Figure 1E). Overall, our data show that Gs signaling and cAMP levels in LN_vs are important determinants of period length. Although previous studies in *Drosophila* implicated cAMP-mediated signaling in circadian rhythms (Levine et al., 1994; Majercak et al., 1997), our data point to the LN_vs as the relevant cellular substrate.

Normal Go Activity in LN_vs Is Required for 24 Hr Rhythms

Next we tested whether other G alpha proteins are also important for circadian behavior. One major class of G proteins is sensitive to pertussis toxin (Ptx), which specifically inhibits Go signaling in flies (Ferris et al., 2006; Katanaev et al., 2005). Since a Gal4 enhancer trap in the *Go* locus gave expression in s-LN_vs (data not shown), we tested whether Go signaling regulates circadian rhythms by expressing a *UAS-Ptx* transgene (Ferris et al., 2006) in LN_vs. The average behavioral period of *Pdf* > *Ptx* flies in DD is 25.2 hr, significantly longer than control flies ($p < 0.001$) (Figure 2A and Table 1). We also used a UAS-Go transgene in which a single amino acid change (G203T) reduces Go affinity for GTP and decreases endogenous Go signaling in a dominant-negative manner (*Go-GDP*) (Katanaev et al., 2005). *Pdf* > *Go-GDP* flies also had ~1-hr-longer period than control

Table 1. Locomotor Rhythms in DD for Flies with Altered Gs and Go Signaling in LN_vs

Genotype	No. of Flies Assayed	% of Arrhythmic Flies	Period (hr) ± SEM	Power ± SEM
Pdf-Gal4	15	0	24.0 ± 0.1	102 ± 23.8
Pdf > Gs-RNAi	31	0	25.0 ± 0.1	113.8 ± 13.0
Pdf > Gs	20	65	24.2 ± 0.2	36.8 ± 9.3
Pdf > Gs-GTP	26	62	24.0 ± 0.1	14.5 ± 2.6
Pdf > dnc	38	0	26.6 ± 0.1	317.1 ± 26.5
Pdf > $Pde8^{EY10946}$	16	6	25.0 ± 0.1	200.3 ± 22.1
UAS-Gs-RNAi / +	27	4	23.8 ± 0.1	75.4 ± 6.8
UAS-Gs / +	19	5	24.5 ± 0.1	76.2 ± 10.9
UAS-Gs-GTP / +	16	6	24.1 ± 0.1	77.3 ± 16.0
UAS-dnc / +	28	0	24.0 ± 0.1	221.8 ± 18.5
$Pde8^{EY10946}$ / +	15	0	24.2 ± 0.1	170.8 ± 17.9
Pdf > Gs-GTP + dnc	20	0	24.7 ± 0.1	197.1 ± 24.7
Pdf > Gs-GTP + CD8::GFP	19	21	23.4 ± 0.3	74.1 ± 10.3
Pdf > Ptx	36	0	25.2 ± 0.1	67.8 ± 6.6
Pdf > Go-GDP	49	4	25.0 ± 0.1	100.8 ± 10.1
Pdf > Go-GTP	26	46	22.3 ± 0.3	24.8 ± 2.3
UAS-Ptx / +	17	12	23.8 ± 0.1	66.9 ± 12.7
UAS-Go-GTP / +	16	0	23.6 ± 0.1	130.1 ± 16.7
UAS-Go-GDP / +	12	0	23.8 ± 0.1	136.5 ± 33.1
Pdf > Go-GTP + CD8::GFP	11	55	22.6 ± 0.2	39.7 ± 10.1
Pdf > Go-GTP + Plc21C-RNAi	22	0	24.7 ± 0.1	199.7 ± 17.9
Pdf > Go-GTP + Gnf1-RNAi	12	17	22.8 ± 0.3	61.4 ± 11.4
Pdf > Go-GTP + dnc	13	23	21.6 ± 0.1	48.5 ± 7.3
Pdf > dnc + Ptx	26	8	28.4 ± 0.1	104.4 ± 14.3
Pdf > Plc21C-RNAi	29	0	25.1 ± 0.1	195.6 ± 17.3
Pdf > Gnf1-RNAi	14	7	24.3 ± 0.1	118.2 ± 10.4
Pdf > $GABA_B$-R2-RNAi (1784)	30	0	24.3 ± 0.1	160.5 ± 10.9
Pdf > $GABA_B$-R2-RNAi (1785)	22	0	24.2 ± 0.1	78.6 ± 8.4
Pdf > $GABA_B$-R3-RNAi	21	0	24.9 ± 0.1	92.5 ± 14.6
UAS-$GABA_B$-R3-RNAi / +	14	0	23.8 ± 0.1	56.7 ± 11.7
UAS-NaChBac2 / +	16	6	24.1 ± 0.1	112.5 ± 18.4
Gad-Gal4 / +	15	7	24.0 ± 0.2	119.4 ± 19.9
Gad > NaChBac2	31	39	24.3 ± 0.3	38.6 ± 5.2

The nomenclature *Pdf > X* indicates that two copies of *$Pdf_{0.5}$-Gal4* (Park et al., 2000) were used to express *UAS-X*. *Pdf > X + Y* indicates simultaneous expression of *UAS-X* and *UAS-Y*. Period is shown in hr for rhythmic flies with standard error of the mean (SEM). Power indicates rhythm strength with its SEM.

flies ($p < 0.001$) (Figure 2A and Table 1). Therefore, inhibiting endogenous Go activity in LN_vs using two independent transgenes lengthened period.

We also assayed behavioral rhythms of flies expressing a constitutively active Go transgene (*Go-GTP*; Katanaev et al., 2005) and found that nearly 50% of *Pdf > Go-GTP* flies were arrhythmic. The remaining rhythmic flies had short period rhythms (22.3 hr), although with a weak power (Figure 2A and Table 1). Thus, reduced signaling via Go in LN_vs lengthens period, whereas increased Go signaling leads to arrhythmicity or short periods.

Plc21C Lies Downstream of *Go* in LN_vs

Unlike Gs, the signaling pathway downstream of Go in *Drosophila* is unclear. One well-studied pathway downstream of G proteins involves PLC enzymes, which cleave the phospholipid PIP2 into second messengers. *Plc21C* is widely expressed in the brain and colocalizes with Go at low resolution (Shortridge et al., 1991).

We hypothesized that the arrhythmicity of *Pdf > Go-GTP* flies should be rescued by reducing downstream signaling as observed with coexpression of *UAS-dnc* with *UAS-GsGTP* (Figure 1C). Therefore, we measured locomotor rhythms of flies expressing *UAS-Go-GTP* in LN_vs along with either *UAS-dnc* or with an RNAi transgene that targets *Plc21C*. To control for transgene expression levels, we also assayed flies with *Go-GTP* coexpressed with GFP or RNAi to *Germ line transcription factor 1* (*Gnf1*), which is unlikely to be expressed in LN_vs. The results in Figure 2B and Table 1 show that *Pdf > Go-GTP + GFP* and *Pdf > Go-GTP + Gnf1-RNAi* flies were either arrhythmic or had weak rhythms.

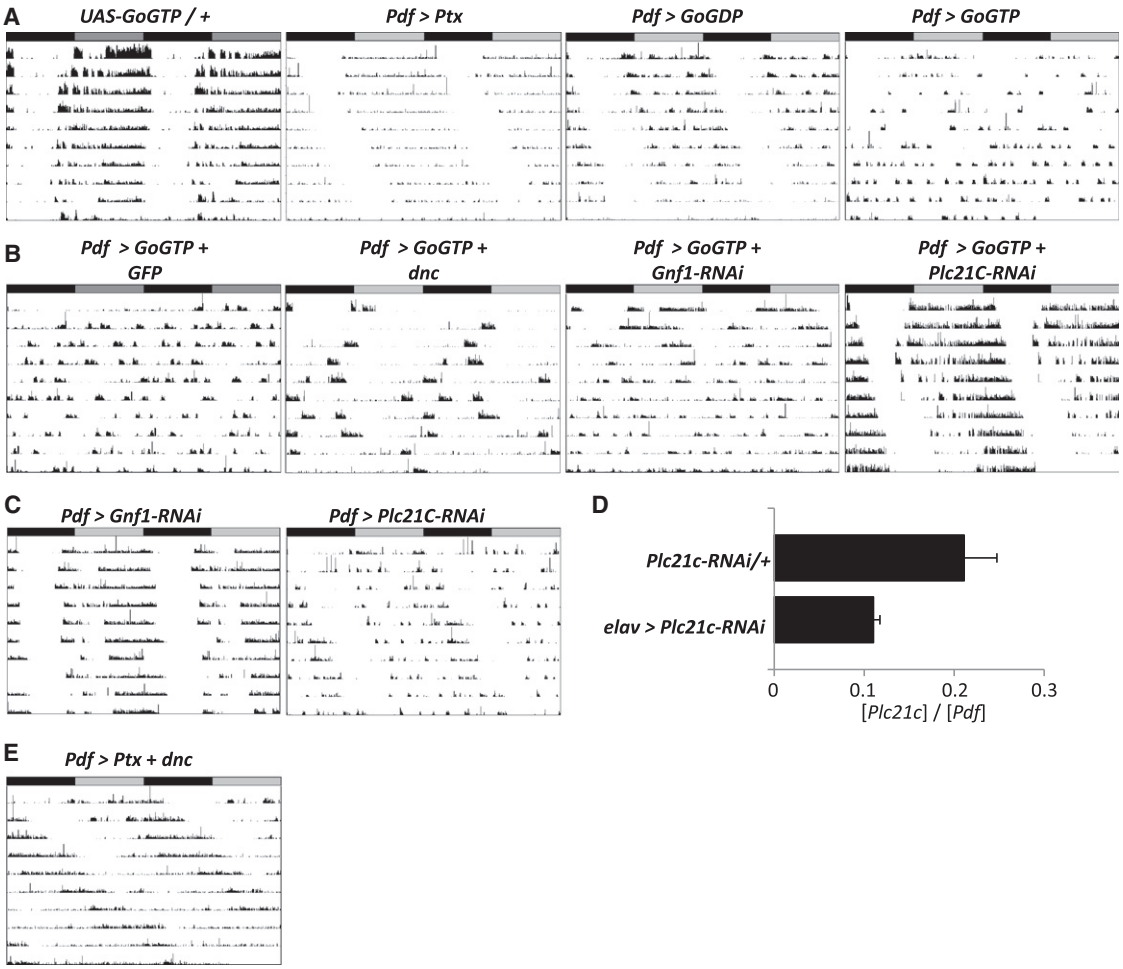

Figure 2. Go Signaling in LN_vs Requires *Plc21C* for 24 Hr Behavioral Rhythms

Representative actograms for flies in DD as in Figure 1.

(A) Left: A control fly heterozygous for a constitutively active *Go* transgene (*UAS-Go-GTP* / +, 23.6 hr). The next panels (left to right) show activity of flies with *Pdf-Gal4* expressing transgenes with Pertussis toxin (*Pdf* > *Ptx*, 25.2 hr), constitutively inactive *Go* (*Pdf* > *Go-GDP*, 25.0 hr) or constitutively active *Go* (*Pdf* > *Go-GTP*). *Pdf* > *Ptx* and *Pdf* > *Go-GDP* flies had significantly longer rhythms than controls ($p < 0.001$ versus *Pdf-Gal4*). *Pdf* > *Go-GTP* flies either became arrhythmic during DD or had shorter rhythms than control flies (22.3 hr, $p < 0.001$ versus *Pdf-Gal4* and *UAS-Go-GTP* / + flies).

(B) *Pdf* > *Go-GTP* flies expressing a third transgene. From left to right: *UAS-CD8::GFP* control (*Pdf* > *Go-GTP* + *GFP*), *UAS-dnc* (*Pdf* > *Go-GTP* + *dnc*), control RNAi to *Gnf1* (*Pdf* > *Go-GTP* + *Gnf1-RNAi*), and RNAi to *Plc21C* (*Pdf* > *Go-GTP* + *Plc21C-RNAi*). *Pdf* > *Go-GTP* + *Plc21C-RNAi* flies had stronger rhythms than *Pdf* > *Go-GTP* + *Gnf1-RNAi* flies ($p < 0.001$).

(C) Flies with a control RNAi (*Pdf* > *Gnf1-RNAi*, 24.3 hr, left) or RNAi against *Plc21C* (*Pdf* > *Plc21C*, 25.1 hr, right). *Pdf* > *Plc21C-RNAi* flies have longer periods than control flies ($p < 0.001$ versus *Pdf* > *Gnf1*).

(D) qPCR on RNA isolated from adult fly heads from either *UAS-Plc21C-RNAi* / + heterozygotes or flies with *elav-Gal4* expressing *UAS-Plc21C-RNAi* in postmitotic neurons (*elav* > *Plc21C-RNAi*). The relative levels of *Plc21C* and *Pdf* RNA are plotted with error bars showing SEM. *elav* > *Plc21C-RNAi* flies have less *Plc21C* RNA than controls ($p = 0.05$).

(E) Locomotor activity of a fly coexpressing *UAS-dnc* and *UAS-Ptx* in LN_vs (*Pdf* > *dnc* + *Ptx*). *Pdf* > *dnc* + *Ptx* flies had longer periods (28.4 hr) than *Pdf* > *dnc* and *Pdf* > *Ptx* flies ($p < 0.001$).

Pdf > *Go-GTP* + *dnc* flies had low power short-period rhythms, indicating that Go is unlikely to signal by increasing cAMP in LN_vs. This finding is consistent with Go acting independently of the cAMP pathway in mushroom bodies (Ferris et al., 2006). Strikingly, all *Pdf* > *Go-GTP* + *Plc21C-RNAi* flies had strong rhythms. Since *Plc21C-RNAi* suppressed the *Go-GTP* phenotype, we conclude that *Plc21C* lies downstream of *Go* in LN_vs.

We noticed that *Pdf* > *Go-GTP* + *Plc21C-RNAi* flies had slightly longer period rhythms (24.7 hr) than control flies. *Pdf* > *Plc-21C-RNAi* flies without Go-GTP also have a longer period (25.1 hr) than control *Pdf* > *Gnf1-RNAi* flies (Figure 2C and Table1), consistent with the long periods seen when Go activity is reduced in LN_vs. We confirmed that the *UAS-Plc21c-RNAi* transgene reduced *Plc21C* RNA levels when expressed pan-neuronally (Figure 2D). Thus, the Go / PLC21C signaling pathway helps LN_vs drive 24 hr behavioral rhythms.

These data indicate that Go and Gs activate distinct signaling pathways. Since combining two mutations that affect different

steps in the molecular clock affects period length additively (Lakin-Thomas and Brody, 1985; Rothenfluh et al., 2000), we tested whether Go and Gs pathways act in parallel by measuring the period lengths of flies with both pathways inhibited simultaneously. We found that flies coexpressing *dnc* and *Ptx* in LN_vs have an average period of 28.4 hr, significantly longer than either *Pdf* > *dnc* or *Pdf* > *Ptx* flies alone ($p < 0.001$; Figure 2D and Table 1). Therefore, we conclude that Gs and Go signaling act in parallel in LN_vs to promote 24 hr rhythms.

Inhibiting Go Slows the Molecular Clock

Altered period behavioral rhythms are typically associated with changes in the s-LN_v molecular clock. To test this for Go signaling, we assayed molecular clock oscillations in *Pdf* > *Ptx* flies. We dissected adult flies on the third day of DD so that the 1.3 hr difference in period length per day would result in a ~4 hr shift. We stained fly brains at 4 hr intervals for the rhythmically produced clock protein VRI, which is detected during subjective night in wild-type flies (Cyran et al., 2003; Glossop et al., 2003).

VRI staining was first detected in control s-LN_vs at CT16, reached peak levels at CT20, and then became almost undetectable by CT24. In contrast, VRI was not clearly detectable in s-LN_vs of *Pdf* > *Ptx* flies until CT20 and remained at high levels at CT24, before disappearing by CT4 on the next day (Figure 3). Therefore, the s-LN_v molecular clock in *Pdf* > *Ptx* flies is rhythmic, but its phase is delayed, consistent with long period behavioral rhythms. Thus, Go-PLC21C signaling interacts with core clock components to regulate molecular clock speed.

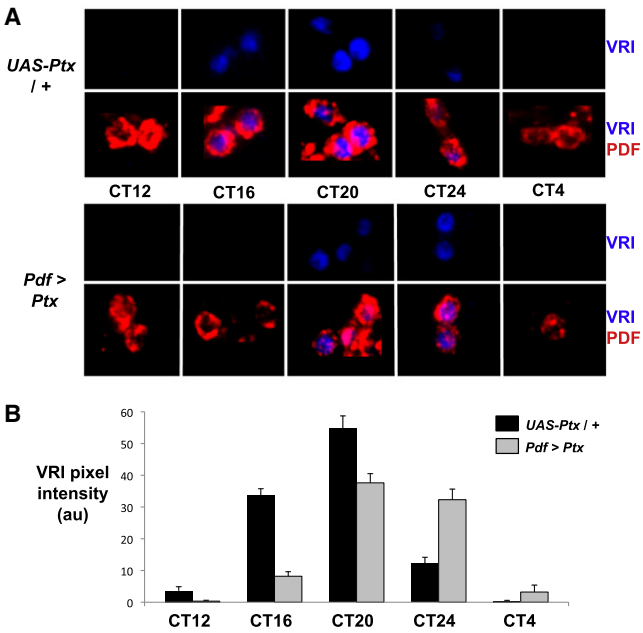

Figure 3. Molecular Clock Progression Is Delayed by Inhibiting Go Signaling

(A) Representative confocal images of s-LN_vs on days 3–4 in DD stained for VRI (blue) and PDF (red) in *UAS-Ptx* / + control flies (top panels) and *Pdf* > *Ptx* flies (bottom).

(B) Data are quantified for *UAS-Ptx* / + controls (black) and *Pdf* > *Ptx* (gray) with error bars showing SEM.

Go Is Required for GABA to Inhibit LN_v Neuronal Activity In Vitro

Although LN_vs are usually considered cell-autonomous oscillators, the involvement of Gs and Go signaling suggested that they normally receive inputs to generate 24 hr rhythms. Given that Go signaling was previously unstudied in fly circadian rhythms, we sought to identify ligands and GPCRs that signal via Go in LN_vs as the first step toward identifying the neurons that help set molecular clock speed.

For this, we modified the assay of Wegener et al. (2004) that measures Ca^{2+} responses in dissociated larval LN_vs. We used larval LN_vs to be able to use the strong *Pdf-Gal4* driver without needing to distinguish s- and l-LN_vs by size. Studying larval LN_vs is relevant because they become the adult s-LN_vs (Kaneko et al., 1997), and gene expression patterns remain similar between larval LN_vs and adult s-LN_vs (Nagoshi et al., 2010).

Instead of measuring Ca^{2+} changes via Fura-2, we used the genetically encoded Ca^{2+} indicator *G-CaMP1.6* (Reiff et al., 2005). We found that larval LN_vs expressing G-CaMP fluoresce more reliably and strongly than after Fura-2 loading; 10 μM ACh robustly increased fluorescence (25%–80% of baseline) in >90% of G-$CaMP^+$ dissociated LN_vs, as previously described (Wegener et al., 2004). Fluorescence did not run down during an experiment (Figure 4A; Figures S2 and S3) allowing a single G-$CaMP^+$ neuron to be recorded for >30 min.

We found a similar concentration-response relationship for ACh in G-$CaMP^+$ neurons as Wegener et al. (2004) had found for Fura-2 loaded LN_vs (Figure 4C). These Ca^{2+} increases require nicotinic ACh receptor (nAChR) activation since 10 μM nicotine also increased G-CaMP fluorescence (Figure S2A), as reported by Wegener et al. (2004). Furthermore, applying the nAChR antagonist α-Bungarotoxin (α-Btx) prevented intracellular Ca^{2+} increases when coapplied with ACh (Figure S2A; M. Vömel and C. Wegener, personal communication). α-Btx inhibition on LN_vs was reversible (Figure S2A) as previously described in insect cells (Albert and Lingle, 1993).

In agreement with Wegener et al. (2004), we also found that ACh-induced intracellular Ca^{2+} increases require extracellular Ca^{2+} (Figure S2B) and are blocked by 30 μM extracellular Cd^{2+}, which inhibits voltage-gated Ca^{2+} channels (VGCC) (Figure S2C). Raising extracellular K^+ to depolarize LN_vs also increased G-CaMP fluorescence to similar levels as ACh (EC_{50} for K^+, 30.8 ± 1.2 mM) (Figure S3A and data not shown). These data indicate that ACh binds to nAChRs that activate VGCC to allow extracellular Ca^{2+} to enter LN_vs. For this, nAChRs and VGCCs must be in close proximity at least in dissociated larval LN_vs, and this system offers a powerful way to study the direct effects of ligands on LN_vs.

We tested a number of other neurotransmitters but found no change in G-CaMP fluorescence in LN_vs either during or after applications of 100 μM GABA, glutamate, glycine, histamine, 5-HT, NMDA, or octopamine (data not shown). These high neurotransmitter doses would be expected to give responses if LN_vs possess the appropriate receptors. However, it was previously reported that glutamate and GABA decrease Ca^{2+} levels via metabotropic glutamate and GABA receptors ($GABA_B$-Rs)

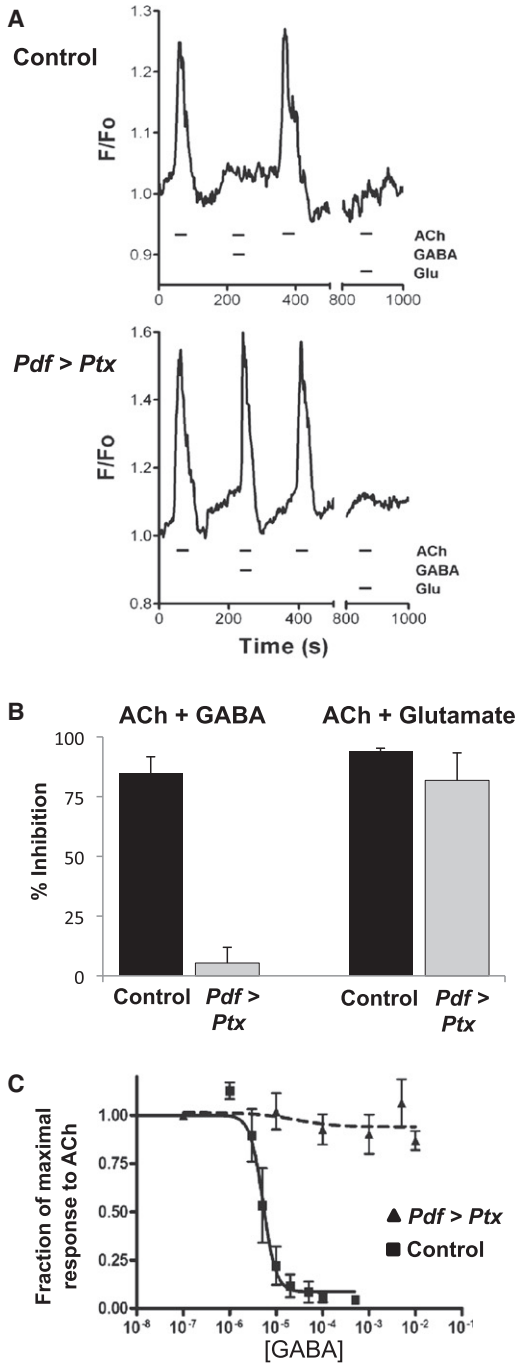

Figure 4. Go Is Required for the Inhibitory Effects of GABA on Larval LN_vs

(A) Representative fluorescence measurements from dissociated larval LN_vs when 10 μM acetylcholine (ACh) was applied alone or together with 100 μM GABA or glutamate (Glu). Upper traces are LN_vs with *Pdf-Gal4* expressing *UAS-G-CaMP* (Control). Lower traces are LN_vs with *Pdf-Gal4* expressing *UAS-G-CaMP* and *UAS-Ptx* (*Pdf* > *Ptx*).

(B) Quantitation of inhibition by GABA (left) or glutamate (right) of 10 μM ACh-induced Ca^{2+} responses for control (black) and *Pdf* > *Ptx* (gray) LN_vs. Error bars show SEM. Ptx prevented GABA-mediated inhibition ($p < 0.001$ versus *Pdf* > *G-CaMP*; n = 9) but had no effect on glutamate inhibition ($p > 0.2$; n = 5).

in Fura-2 loaded LN_vs (Hamasaka et al., 2005, 2007). These receptors are candidates for coupling to Go. Since we could not detect spontaneous activity with GABA and glutamate in dissociated LN_vs, we coapplied them with ACh to attempt to detect inhibition. We found that coapplying 100 μM GABA or glutamate almost completely inhibited the Ca^{2+} response to 10 μM ACh (Figures 4A and 4B).

To test whether Go is required for inhibition by GABA and/or glutamate, we compared the responses of control *Pdf* > *G-CaMP* larval LN_vs with LN_vs also expressing *UAS-Ptx* (*Pdf* > *G-CaMP* + *Ptx*). Both sets of cells responded similarly to ACh applied alone (Figures 4A and 4B). When ACh was coapplied with 100 μM GABA, the response of control *Pdf* > *G-CaMP* LN_vs was inhibited by 85%. However, the inhibition by GABA was only 5% in *Pdf* > *G-CaMP* + *Ptx* cells (Figures 4A and 4B). We estimated the GABA IC_{50} for control LN_vs as 3.8 μM, whereas GABA did not inhibit the ACh response of *Pdf* > *G-CaMP* + *Ptx* LN_vs even at 10 mM (Figure 4C). Coapplying glutamate with ACh inhibited the ACh-induced Ca^{2+} response in both sets of cells (Figures 4A and 4B), indicating that Ptx specifically blocks GABA-mediated inhibition. Since Ptx prevents the Go-α/β/γ heterotrimer from coupling to activated GPCRs, we propose that metabotropic $GABA_B$-Rs normally signal via Go in LN_vs. Similar conclusions were made in *Drosophila* olfactory receptor neurons using *UAS-Ptx* (Olsen and Wilson, 2008).

Adult l-LN_vs have functional $GABA_A$/RDL receptors that are sensitive to picrotoxin and are implicated in arousal (Chung et al., 2009; Parisky et al., 2008). However, we found that 4 μM picrotoxin, which blocks the open channel of $GABA_A$/RDL receptors, did not alter GABA inhibition of ACh-induced Ca^{2+} responses in larval LN_vs (Figure S3C). Thus, the GABA-mediated inhibition observed here is independent of $GABA_A$/RDL receptors. The general K^+ channel inhibitors TEA or Cs^+ (Hille, 2001) did not affect GABA-mediated inhibition (Figure S3C). Although the sequence of one of the three *Drosophila* G protein-coupled Inward Rectifier K^+ channel suggests that it may not be blocked by TEA (Kavanaugh et al., 1991; McCormack, 2003), the lack of an effect of Cs^+ is consistent with GABA inhibiting LN_vs independently of K^+ channels.

GABA Signals via $GABA_B$-R3 Receptors in LN_vs

Next we sought to identify the $GABA_B$ receptor(s) in LN_vs responsible for GABA inhibition of ACh. The *Drosophila* genome has three annotated $GABA_B$-R genes (Mezler et al., 2001): $GABA_B$-R1 and $GABA_B$-R2 form a functional heterodimer, whereas $GABA_B$-R3 does not dimerize with $GABA_B$-R1 or R2 and probably interacts with an as yet unidentified additional $GABA_B$-R (Kaupmann et al., 1998; Mezler et al., 2001).

To identify which $GABA_B$ receptor(s) is required in LN_vs, we first used 3-APMPA, an agonist for *Drosophila* $GABA_B$-R1/2 (Hamasaka et al., 2005; Mezler et al., 2001). 3-APMPA did not alter LN_v Ca^{2+} responses when coapplied with ACh, even at 20 μM (data not shown), which is more than twice the reported

(C) Dose-response curve for GABA on control (squares, solid line) and *Pdf* > *Ptx* (triangles, dashed line) LN_vs. Error bars show SEM. IC_{50} for control LN_vs is 3.8 μM but was unmeasurable for *Pdf* > *Ptx* LN_vs.

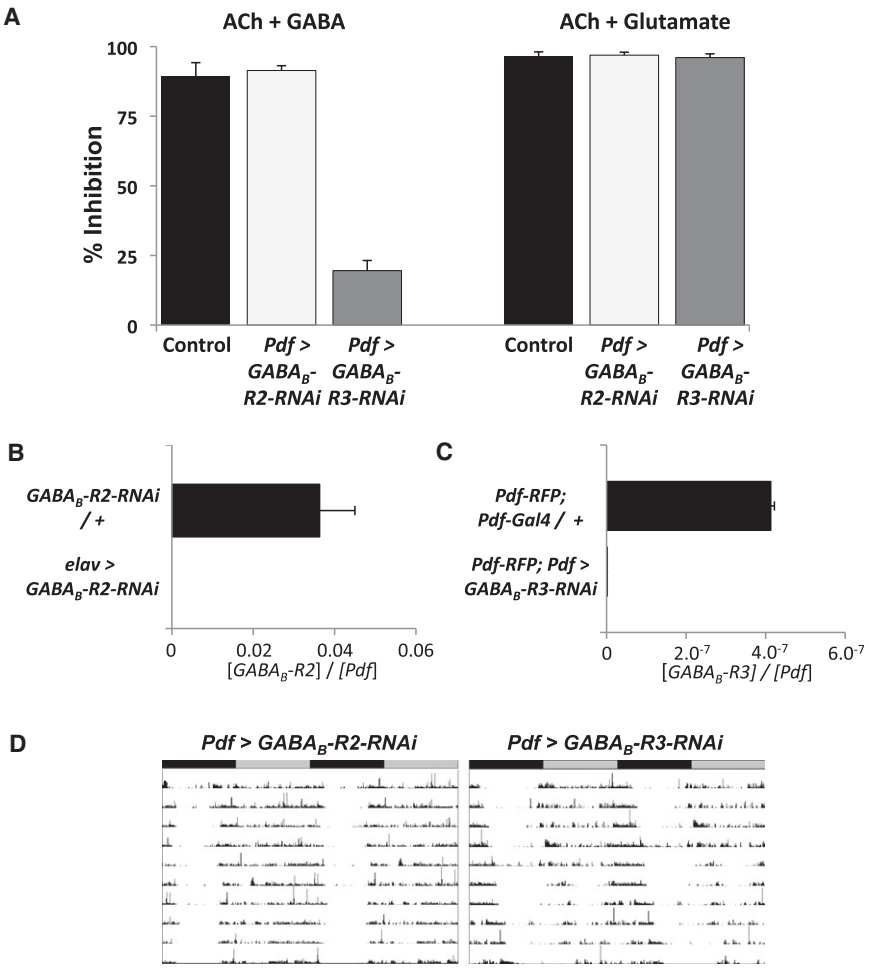

Figure 5. RNAi to the Metabotropic GABA Receptor GABA$_B$-R3 Subunit Reduces Inhibition by GABA and Lengthens Period of Adult Locomotor Rhythms

(A) Quantification of inhibition of Ca^{2+} responses for ACh + GABA (left) or ACh + glutamate (right) compared to ACh. Error bars show SEM. LN$_v$s from larvae with *Pdf-Gal4* and *UAS-G-CaMP* and either no other transgenes (control, black bars, 89% inhibition), *UAS-GABA$_B$-R2-RNAi* on Chr. III (*Pdf > GABA$_B$-R2-RNAi*, light gray, 91% inhibition, $p > 0.5$ versus control) or *UAS-GABA$_B$-R3-RNAi* (*Pdf > GABA$_B$-R3-RNAi*, dark gray, 19.5% inhibition, $p < 0.001$ versus control).

(B) Adult head RNA levels of *GABA$_B$-R2* and *Pdf* were measured as in Figure 2 from either *UAS-GABA$_B$-R2-RNAi* heterozygotes (*GABA$_B$-R2-RNAi / +*) or flies with *elav-Gal4* expressing *UAS-GABA$_B$-R2-RNAi* (*elav > GABA$_B$-R2-RNAi*). *GABA$_B$-R2* RNA levels were lower in *elav > GABA$_B$-R2-RNAi* flies ($p < 0.01$). Error bars show SEM.

(C) *GABA$_B$-R3* and *Pdf* RNA levels measured by qPCR on amplified RNA from adult LN$_v$s isolated from *Pdf-RFP; Pdf-Gal4 / +* controls or flies which also had *UAS-GABA$_B$-R3-RNAi* (*Pdf-RFP; Pdf > GABA$_B$-R3-RNAi*). *GABA$_B$-R3* RNA levels were reduced in *Pdf-RFP; Pdf > GABA$_B$-R3-RNAi* flies ($p < 0.02$). *Pdf* RNA levels were ~2.5-fold higher with *GABA$_B$-R3-RNAi* flies and so the extent of knockdown with this RNAi transgene (>400-fold) may be overestimated.

(D) Representative actograms of adult flies expressing either *GABA$_B$-R2-RNAi* (*Pdf > GABA$_B$-R2-RNAi*, left) or *GABA$_B$-R3-RNAi* (*Pdf > GABA$_B$-R3-RNAi*, right) in LN$_v$s. *Pdf > GABA$_B$-R3-RNAi* flies have longer period rhythms than *Pdf > GABA$_B$-R2-RNAi* flies (24.9 hr versus 24.3 hr; $p < 0.001$).

3-APMPA EC_{50} (Hamasaka et al., 2005). GABA also inhibited LN$_v$ Ca^{2+} responses to ACh when LN$_v$s expressed a *UAS-GABA$_B$-R2-RNAi* transgene (Figure 5A) even though this *GABA$_B$-R2-RNAi* transgene potently reduces *GABA$_B$-R2* expression (Figure 5B). Since GABA$_B$-R1 and GABA$_B$-R2 seem to function together, we conclude that GABA$_B$-R1/2 is not involved in GABA-mediated inhibition of ACh responses in LN$_v$s.

GABA$_B$-R3 expression is enriched ~20-fold in adult s-LN$_v$s at ZT12 compared to other differentiated neurons (Kula-Eversole et al., 2010). To test a role for GABA$_B$-R3 in mediating GABA responses in LN$_v$s, we used a *UAS-GABA$_B$-R3-RNAi* transgene since there are no pharmacological agents that target GABA$_B$-R3. We compared the responses of LN$_v$s from control *Pdf > G-CaMP* larvae and from larvae expressing both *G-CaMP* and *GABA$_B$-R3-RNAi* transgenes. The results in Figure 5A and Figures S3A and S3B show normal activation by ACh and inhibition by glutamate. However, although GABA inhibited the response of control *Pdf > G-CaMP* LN$_v$s to ACh by 89%, *Pdf > G-CaMP + R3-RNAi* LN$_v$s showed only 20% inhibition. We could not detect a significant change in *GABA$_B$-R3* expression in RNA from whole fly heads when *GABA$_B$-R3-RNAi* was expressed with *elav-Gal4*. Instead, we measured *GABA$_B$-R3* RNA levels from adult LN$_v$s purified via flow cytometry using a *Pdf-RFP* transgene (Blanchard et al., 2010) to sort LN$_v$s. This technique reliably reports rhythmic clock gene expression in LN$_v$s (M.R., M. Drapeau, and J.B., unpublished data). The RNA analyzed is probably from a mixture of s- and l-LN$_v$s. The results in Figure 5C show that *GABA$_B$-R3* RNA levels are significantly higher in LN$_v$s isolated from *Pdf-RFP* control flies than in LN$_v$s from *Pdf-RFP; Pdf > GABA$_B$-R3-RNAi* flies. Therefore, the *GABA$_B$-R3-RNAi* transgene reduces *GABA$_B$-R3* expression. Overall, our data indicate that GABA$_B$-R3 is the relevant GABA$_B$ receptor that mediates the inhibitory effects of GABA on LN$_v$ Ca^{2+} responses.

To test whether reducing expression of *GABA$_B$-R3* alters adult behavioral rhythms, we assayed the locomotor activity of flies expressing RNAi against *GABA$_B$-R3* in adult LN$_v$s and compared them to flies expressing *GABA$_B$-R2-RNAi*. The results in Figure 5D and Table 1 show that *Pdf > GABA$_B$-R3-RNAi* flies had longer periods than did *Pdf > GABA$_B$-R2-RNAi* flies (24.9 hr versus 24.3 hr, respectively; $p < 0.001$). The long period is consistent with reduced signaling via Go in *Pdf > Ptx* and *Pdf > Go-GDP* flies (Table1). Taken together, our results indicate that signaling via GABA$_B$-R3 in s-LN$_v$s helps to generate 24 hr

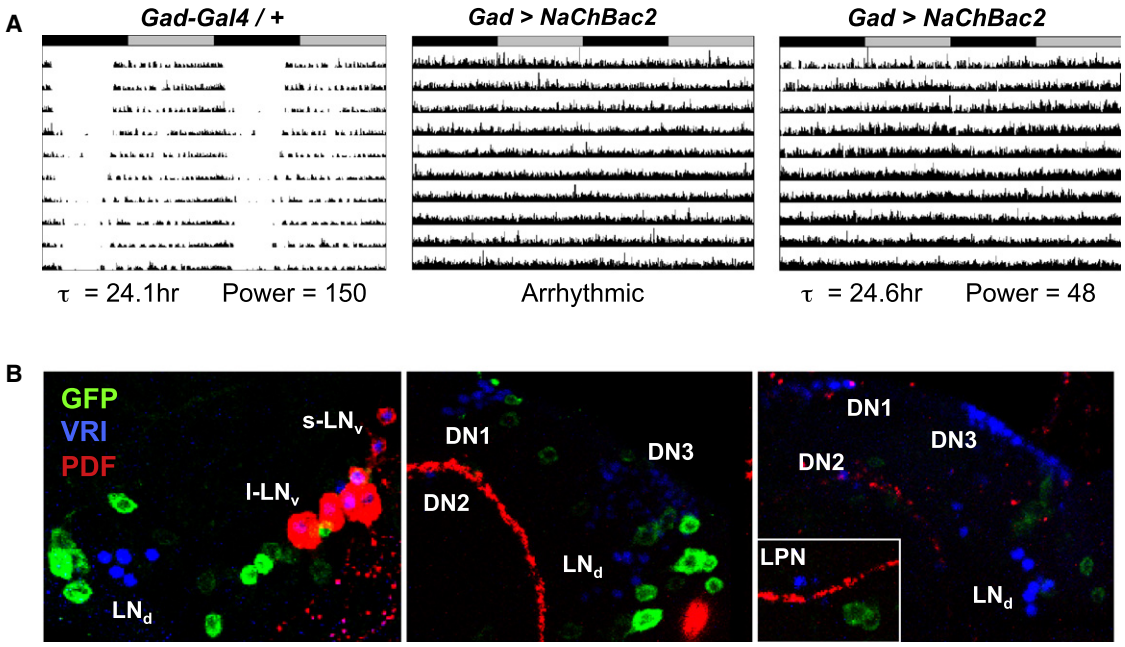

Figure 6. Hyperexciting GABAergic Neurons Causes Behavioral Arrhythmicity

(A) Representative actograms of heterozygous control *Gad-Gal4* / + fly (left) and two flies with *Gad-Gal4* expressing *UAS-NaChBac2* (*Gad* > *NaChBac2*, center and right). ClockLab marked the *Gad* > *NaChBac2* center fly as arrhythmic and the fly on the right as having a period of 24.6 hr and a low-power rhythm. Rhythmic *Gad* > *NaChBac2* flies had weaker power rhythms then control flies ($p < 0.001$).

(B) Localization of *Gad-Gal4* expression using a *UAS-CD8::GFP* reporter in three individual brains stained at ZT20 with antibodies to GFP (green), VRI (blue, marks all clock neurons), and PDF (red). Although some GFP^+ neurons are close to VRI^+ clock neurons, there is no obvious colocalization of VRI and GFP. Images are representative of 13 brain lobes.

rhythms and raise the possibility that GABAergic neurons are part of the circadian network.

Hyperexciting GABAergic Neurons Disrupts Circadian Rhythms

Given the presence of functional $GABA_B$-R3 receptors in LN_vs, we asked whether manipulating GABAergic neurons themselves also affects circadian rhythms. We used two Gal4 drivers with regulatory regions from *Glutamate decarboxylase 1 (Gad1)*, which encodes the enzyme that converts Glutamate into GABA, and one with the regulatory region of the *vesicular GABA transporter* (*vGAT*; Fei et al., 2010). However, these GABAergic neuron drivers were mainly lethal when crossed to transgenes that ablate, hyperpolarize, or hyperexcite neurons or block synaptic release. However, healthy offspring were obtained by crossing *Gad-Gal4* (Mehren and Griffith, 2006) to *UAS-NaChBac2*, which encodes a voltage-gated bacterial Na^+ channel that hyperexcites neurons (Nitabach et al., 2006; Sheeba et al., 2008). The results in Figure 6A and Table 1 show that *Gad* > *NaChBac2* flies were either arrhythmic or had significantly weaker rhythms than control flies.

To test whether these behavioral phenotypes are due to expression in clock neurons, we crossed *Gad-Gal4* with *GFP* reporter flies. We could not detect GFP expression in any clock neurons (Figure 6B), consistent with no GABA immunoreactivity in clock neurons (Hamasaka et al., 2005). Therefore, the disrupted locomotor rhythms in *Gad* > *NaChBac2* flies are due to hyperexciting *Gad-Gal4* expressing cells that are not canonical clock neurons.

Altering GABAergic neuron activity changes *Drosophila* sleep levels in LD cycles (Agosto et al., 2008; Parisky et al., 2008). Therefore, the altered behavioral rhythms of *Gad* > *NaChBac2* flies could result from altered arousal mediated via GABAergic neurons. In this scenario, the s-LN_v molecular clocks would be expected to run normally in *Gad* > *NaChBac2* flies. Alternatively, the weak behavioral rhythms of *Gad* > *NaChBac2* flies could be at least partly due to increased GABAergic signaling that alters s-LN_v molecular clocks.

To assay the s-LN_v molecular clock, we compared levels of the clock proteins VRI and PER in s-LN_vs of *Gad-Gal4* control flies and *Gad* > *NaChBac2* flies at four different time points on day 3 in DD. Figure 7 shows that overall VRI and PER levels are lower in *Gad* > *NaChBac2* flies than in control flies. Furthermore, VRI and PER levels are variable between s-LN_vs in the same cluster in *Gad* > *NaChBac2* brains. For example, VRI was detected in only two of the four s-LN_vs in the *Gad* > *NaChBac2* fly shown at CT3 (Figure 7A). We also measured VRI and PER levels in LD cycles and found no significant difference between control and experimental flies (data not shown), indicating that s-LN_vs entrain properly and that light overrides the effect of hyperexciting GABAergic neurons. Since molecular rhythms in s-LN_vs are disrupted by hyperexciting GABAergic neurons, we conclude that normal levels of signaling from GABAergic neurons are necessary for 24 hr molecular clock rhythms in s-LN_vs in DD.

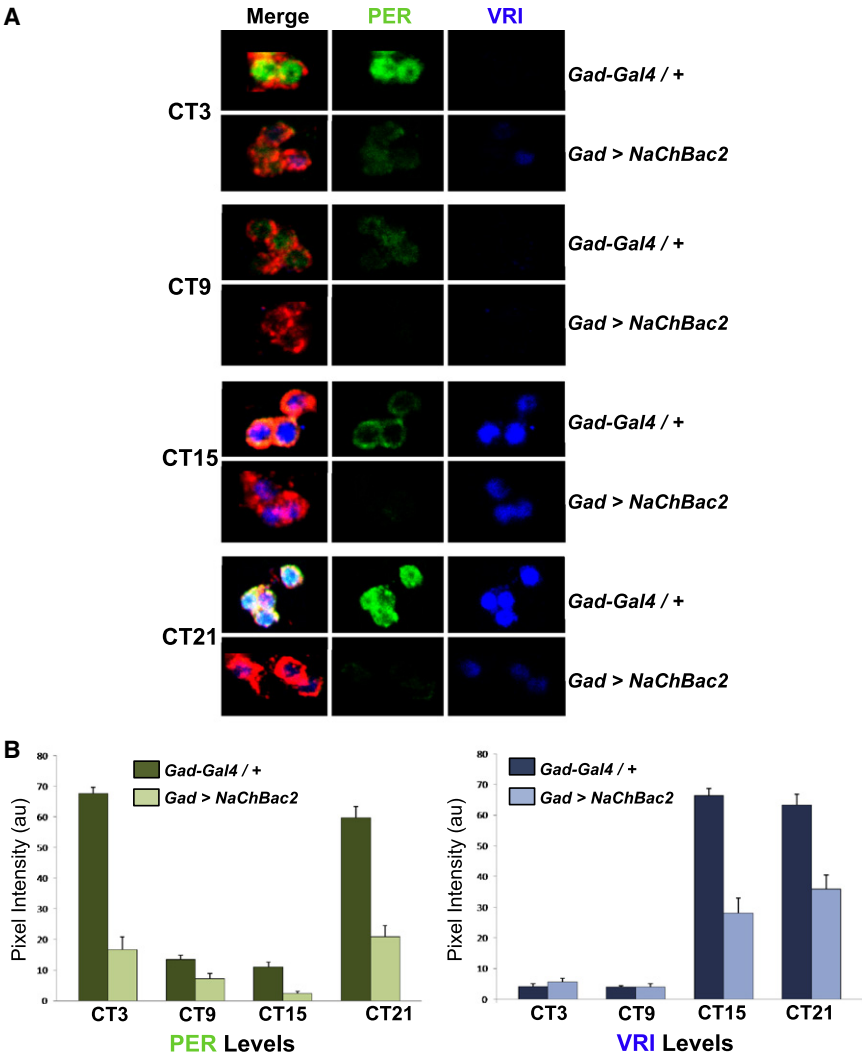

Figure 7. Hyperexciting GABAergic Neurons Disrupts s-LN$_v$ Molecular Rhythms

(A) Representative confocal images of s-LN$_v$s at four time points on day 3 in DD using antibodies to PER (green), VRI (blue), and PDF (red) in *Gad-Gal4* / + control flies (top panels) and *Gad* > *NaChBac2* flies (bottom panels).

(B) Data are quantified for *Gad-Gal4* / + controls (dark green and dark blue bars for PER and VRI respectively) and for *Gad* > *NaChBac2* (light green and light blue) with error bars showing SEM. Experiments were performed on 3 separate days with at least 12 brains and 30 clearly identifiable s-LN$_v$s measured in total.

DISCUSSION

G Protein Signaling in LN$_v$s

Here, we demonstrate the importance of G protein signaling in s-LN$_v$s for 24 hr rhythms in DD. We show that Gs and Go pathways act in parallel to regulate the s-LN$_v$ molecular clock, since simultaneously reducing signaling via Gs and Go lengthens rhythms by more than 4 hr. Therefore, LN$_v$s normally require an appropriate level of signaling via Gs and Go to generate 24 hr rhythms in DD. Since activation of Gs and Go generates intracellular second messengers, our work adds to the evidence implicating small molecules in regulating molecular clocks across species (Dodd et al., 2007; Harrisingh et al., 2007; O'Neill et al., 2008).

Signaling via Gs in LN$_v$s

The long periods we observed with reduced Gs signaling are consistent with four other manipulations of cAMP levels or PKA activity that alter fly circadian behavior. First, long-period rhythms with *dnc* overexpression complement the short periods of *dnc* hypomorphs (Levine et al., 1994) and suggest that the latter are due to loss of *dnc* from LN$_v$s. *dnc* mutants also increase phase shifts to light in the early evening. However, we found no difference in phase delays or advances between *Pdf* > *dnc* and control flies (data not shown), suggesting that altered light-responses of *dnc* hypomorphs are due to *dnc* acting in other clock neurons. The period-altering effects we see when manipulating cAMP levels are also consistent with data from Shafer et al. (2008), who found that expressing the cAMP-binding domain of mammalian Epac1 in LN$_v$s lengthens period. This Epac1 domain probably reduces free cAMP levels in LN$_v$s, although presumably not as potently as *UAS-dnc*. Third, mutations in PKA catalytic or regulatory subunits that affect the whole fly disrupt circadian behavior (Levine et al., 1994; Majercak et al., 1997; Park et al., 2000). Fourth, overexpressing a PKA catalytic subunit in LN$_v$s rescues the period-altering effect of a *UAS-shibire* transgene that alters vesicle recycling, although the PKA catalytic subunit had no effect by itself (Kilman et al., 2009). The long periods we observed with reduced Gs signaling in LN$_v$s also parallel mammalian studies in which pharmacologically reducing Adenylate cyclase activity lengthened period in SCN explants and mice (O'Neill et al., 2008).

G proteins typically transduce extracellular signals. What signals could activate Gs in s-LN$_v$s? PDF is one possibility, since PDFR induces cAMP signaling in response to PDF in vitro, indicating that it probably couples to Gs (Hyun et al., 2005; Lear et al., 2005). PDF could signal in an autocrine manner since PDFR is present in LN$_v$s (Im and Taghert, 2010). However, the long periods we observed with reduced Gs signaling differ from the short-period and arrhythmic phenotypes of *Pdf* and *pdfr* mutants. The likeliest explanation for these differences is that the altered behavior of *Pdf* and *pdfr* mutants results from effects of PDF signaling over the entire circadian circuit (Peng et al., 2003; Shafer et al., 2008), whereas our manipulations

specifically targeted LN_vs. Indeed, LN_vs are not responsible for the short-period rhythms in Pdf^{01} null mutant flies (Yoshii et al., 2009). Other possible explanations for the differences between the long-period rhythms with decreased Gs signaling in LN_vs and the short-period rhythms of *Pdf* and *pdfr* mutants are that additional GPCRs couple to Gs in s-LN_vs and influence molecular clock speed and that our manipulations decrease rather than abolish reception of PDF. In summary, our data show that Gs signaling via cAMP in s-LN_vs modulates period length.

Go and GABAergic Signaling Help Generate 24 Hr Periods

Go signaling via PLC21C constitutes a previously unappreciated pathway that regulates the s-LN_v molecular clock. We found that Go and the metabotropic $GABA_B$-R3 receptor are required for the inhibitory effects of GABA on larval LN_vs, which develop into adult s-LN_vs (Kaneko et al., 1997). The same genetic manipulations that block GABA inhibition of LN_vs in culture (expression of *Ptx* or *$GABA_B$-R3-RNAi*) lengthened the period of adult locomotor rhythms. Furthermore, the molecular clock in s-LN_vs is disrupted when a subset of GABAergic neurons are hyperexcited. Since the LN_vs do not produce GABA themselves (Hamasaka et al., 2005 and Figure 6B), s-LN_vs require GABAergic inputs to generate 24 hr rhythms. Thus, s-LN_vs are less autonomous for determining period length in DD than previously anticipated (Stoleru et al., 2005).

Activation of G proteins can have both short- and long-term effects on a cell. With Go signaling blocked by Ptx, we detected short-term effects on LN_v responses to excitatory ACh and longer-term effects on the molecular clock. The latter are presumably explained by PLC activation since the behavioral phenotypes of *Pdf > GoGTP* flies were rescued by reducing *Plc21C* expression.

Since s-LN_v clocks were unchanged even when the speed of all non-LN_v clock neurons were genetically manipulated (Stoleru et al., 2005), it is surprising to find s-LN_v clocks altered by signaling from GABAergic nonclock neurons. Why would LN_vs need inputs from nonclock neurons to generate 24 hr rhythms? One possibility is that LN_vs receive multiple inputs which either accelerate or slow down the pace of their molecular clock but overall balance each other to achieve 24 hr rhythms in DD. Since reducing signaling by Gs and Go lengthens period, these pathways normally accelerate the molecular clock. According to this model, there are unidentified inputs to LN_vs that delay the clock. Identifying additional receptors in LN_vs would allow this idea to be tested.

Previous work showed that GABAergic neurons project to LN_vs (Hamasaka et al., 2005) and that $GABA_A$ receptors in l-LN_vs regulate sleep (Chung et al., 2009; Parisky et al., 2008). Our data show that constitutive activation of Go signaling dramatically alters behavioral rhythms, suggesting that LN_vs normally receive rhythmic GABAergic inputs. But how can s-LN_vs integrate temporal information from non-clock-containing GABAergic neurons? s-LN_vs could respond rhythmically to a constant GABAergic tone by controlling $GABA_B$-R3 activity. Indeed, a recent study found that *$GABA_B$-R3* RNA levels in s-LN_vs are much higher at ZT12 than at ZT0 (Kula-Eversole et al., 2010). Strikingly, this rhythm in *$GABA_B$-R3* expression is in antiphase to LN_v neuronal activity (Cao and Nitabach, 2008; Sheeba et al., 2008). Thus, regulated perception of inhibitory GABAergic inputs could at least partly underlie rhythmic LN_v excitability. GABAergic inputs could also help synchronize LN_vs as in the cockroach circadian system (Schneider and Stengl, 2005). Thus, GABA's short-term effects on LN_v excitability, probably mediated by $G\beta/\gamma$, and GABA's longer-term effects on the molecular clock via Go may both contribute to robust rhythms.

Conclusions

Our work adds to the growing network view of circadian rhythms in *Drosophila* where LN_vs integrate information to set period for the rest of the clock network in DD. The period-altering effects of decreased G protein signaling in LN_vs point to a less hierarchical and more distributed network than previously envisioned. Since our data strongly suggest that GABA inputs regulate circadian rhythms, the GABAergic neurons that fine-tune the s-LN_v clock should be considered part of the circadian network.

EXPERIMENTAL PROCEDURES

Behavioral Analysis

Fly strains used are described in Supplemental Experimental Procedures. For circadian locomotor behavior, flies were loaded into Trikinetics activity monitors and entrained to LD cycles for at least 3 days before transfer to DD. Data were analyzed by ClockLab in conjunction with MatLab. Period length was determined using the Lomb-Scargle algorithm, and power was determined by measuring the height of the peak at this period. Flies with a power >11 had significant rhythms ($p < 0.025$), whereas flies with power <11 were deemed arrhythmic. A two-tailed Student's t test with equal variance was used to test differences in period length.

Immunostaining

Antibodies against PDF (1:50; DSHB), VRI (1:3000; from Paul Hardin), PER (1:5000; from Jeff Hall), and GFP (1:500; AbDSerotec) were used on adult brains, as described elsewhere (Collins et al., 2006). Three experiments were performed on different days with $\geq$8 brains and $\geq$16 clearly identifiable s-LN_vs analyzed per time point. Images were obtained on a Leica SP5 Confocal and Image J used to quantify pixel intensity. Since background staining of VRI and PER was <0.2 au for each condition, background was not subtracted from raw values (range, 2–75), which were pooled and averaged across experiments.

Live-Cell Ca^{2+} Imaging of Dissociated *Drosophila* Clock Neurons

For each experiment, 30–60 third-instar wandering larvae were collected at ZT9 and rinsed in dPBS. Larval brains were dissected, cleaned, rinsed, and placed into dPBS on ice. After two brief rinses in dPBS and gentle centrifugation at 0.2 rcf, brains were resuspended in 400 μl of a 1:1 mixture of dPBS and Schneider's S2 medium (Invitrogen) containing 2 units/mL Dispase II (Roche). After 2 hr at room temperature, brains were washed twice in dPBS, resuspended in 200 μl of S2 medium, and dissociated by pipetting up and down 100 times through a 200 μl pipette tip. Aliquots (50–65 μl) of the cell suspension were placed onto rectangular coverglass (Warner Instruments) and kept in a humidified dark chamber. Cells were allowed at least 2 hr to attach to the coverglass before imaging and were discarded 12 hr after dissection.

The coverglass was mounted on an inverted Nikon TE2000U epifluorescence microscope via a small-volume recording chamber (Warner Instruments). Neurons were illuminated at 480 nm, 6 nm bandpass using a monochromator (Photon Technology International) and were fluorescent emission viewed through a 40×/0.60 Plan Fluor oil-immersion objective (Nikon) and standard FITC filter set (Chroma Technology). Cells were continuously superfused at

2 ml/min with standard saline (Jan and Jan, 1976) using a gravity-driven system. Chemicals were diluted in standard saline, and a manual switching system was used for solution exchange without interrupting flow to cells. Unstimulated G-CaMP-expressing neurons were located by their green emission and subsequent fluorescence summed over 2 s intervals was captured at 12 bit resolution via a CoolsnapFx CCD camera (Roper Scientific). Images were acquired and stored using Imaging Workbench 5.2 (INDEC Biosystems). Ovoid regions of interest were defined entirely within the fluorescent signal within each neuron tested, and time-lapse numerical data obtained during post-hoc playback were exported for further analysis in PRISM 4 (Graphpad). Physiology-grade salts and chemicals were from Fisher Scientific or Sigma Aldrich except for α-bungarotoxin from Tocris.

RNA Analysis

Quantitative real-time RT-PCR (qPCR) was used on RNA isolated at ZT9 from either whole heads or purified adult LN_vs. RNA was extracted using standard procedures for whole fly heads. To isolate RNA from adult LN_vs, brains were dissected starting at ZT9 from adult flies with *Pdf-RFP*, *Pdf-Gal4*, and, for experimental flies, the *UAS-GABA$_B$-R3:RNAi* transgene. Brains were dissociated into a single-cell suspension as for Ca^{2+} imaging above, and a 35-μm nylon mesh filter (BD Falcon) was used to remove cell clusters to minimize contamination by RFP^- cells attached to RFP^+ cells. Cells in Schneider's medium and 10% FBS were kept on ice for transport to NYU School of Medicine FACS center for flow cytometry. We typically obtained ~300 RFP^+ cells from ~50 adult brains, which were sorted directly into 500 μl of PicoPure Extraction Buffer and purified using the PicoPure RNA Isolation Kit (Molecular Devices). mRNA was amplified using the Nugen WT-Ovation Pico System to generate ~5 μg of single stranded amplified unlabeled cDNA product.

For qPCR reactions, 100 ng of adult head RNA or 20 ng of LN_v cDNA was amplified in a Roche LightCycler using the Roche 2-step RT PCR RNA Master HybProbe Kit. RNA levels were determined by comparing when the reaction moved into detectable exponential phase with standard curves for each primer set constructed by reamplifying known quantities of PCR products. We normalized the absolute level of each gene in an experiment to RNA levels of *Pdf* (a noncycling transcript) in that experiment. Three biological replicates were averaged for RNA from whole heads and two for LN_v RNA. Primer and probe sequences are listed in Supplemental Experimental Procedures.

SUPPLEMENTAL INFORMATION

Supplemental Information includes three figures and Supplemental Experimental Procedures and can be found with this article online at doi:10.1016/j.neuron.2010.11.017.

ACKNOWLEDGMENTS

We thank Harold Atwood, Mike Forte, Leslie Griffith, Paul Hardin, Dierk Reiff, Gregg Roman, Julie Simpson, Andrew Tomlinson, Bloomington Stock Center, DSHB, and VDRC for flies and antibodies. We thank Chris Wegener for sharing unpublished data and Gregg Roman and Mike Nitabach for their advice and suggestions. We thank Karim Baroudy, Taniya Kaur, and Alyson Knowles for help in the initial stages of this project and Ben Collins for help with dissections. We also thank Matthieu Cavey, Ben Collins, Alex Keene, Dogukan Mizrak, Afroditi Petsakou, and Daniel Vasiliauskas for comments on the manuscript. Confocal images were obtained in the NYU Center for Genomics & Systems Biology. The investigation was largely conducted in a facility constructed with support from Research Facilities Improvement Grant Number C06 RR-15518-01 from National Center for Research Resources, National Institutes of Health (NIH). The work was supported by NIH grants NS030808 (M.A.) and GM063911 (J.B.).

Accepted: September 24, 2010
Published: December 8, 2010

REFERENCES

Agosto, J., Choi, J.C., Parisky, K.M., Stilwell, G., Rosbash, M., and Griffith, L.C. (2008). Modulation of $GABA_A$ receptor desensitization uncouples sleep onset and maintenance in *Drosophila*. Nat. Neurosci. *11*, 354–359.

Albert, J.L., and Lingle, C.J. (1993). Activation of nicotinic acetylcholine receptors on cultured *Drosophila* and other insect neurones. J. Physiol. *463*, 605–630.

Allada, R., Emery, P., Takahashi, J.S., and Rosbash, M. (2001). Stopping time: the genetics of fly and mouse circadian clocks. Annu. Rev. Neurosci. *24*, 1091–1119.

Balsalobre, A., Damiola, F., and Schibler, U. (1998). A serum shock induces circadian gene expression in mammalian tissue culture cells. Cell *93*, 929–937.

Blanchard, F.J., Collins, B., Cyran, S.A., Hancock, D.H., Taylor, M.V., and Blau, J. (2010). The transcription factor Mef2 is required for normal circadian behavior in *Drosophila*. J. Neurosci. *30*, 5855–5865.

Cao, G., and Nitabach, M.N. (2008). Circadian control of membrane excitability in *Drosophila melanogaster* lateral ventral clock neurons. J. Neurosci. *28*, 6493–6501.

Cheung, U.S., Shayan, A.J., Boulianne, G.L., and Atwood, H.L. (1999). *Drosophila* larval neuromuscular junction's responses to reduction of cAMP in the nervous system. J. Neurobiol. *40*, 1–13.

Chung, B.Y., Kilman, V.L., Keath, J.R., Pitman, J.L., and Allada, R. (2009). The $GABA_A$ receptor RDL acts in peptidergic PDF neurons to promote sleep in *Drosophila*. Curr. Biol. *19*, 386–390.

Collins, B., Mazzoni, E.O., Stanewsky, R., and Blau, J. (2006). *Drosophila* CRYPTOCHROME is a circadian transcriptional repressor. Curr. Biol. *16*, 441–449.

Cyran, S.A., Buchsbaum, A.M., Reddy, K.L., Lin, M.C., Glossop, N.R., Hardin, P.E., Young, M.W., Storti, R.V., and Blau, J. (2003). *vrille, Pdp1*, and *dClock* form a second feedback loop in the *Drosophila* circadian clock. Cell *112*, 329–341.

Day, J.P., Dow, J.A., Houslay, M.D., and Davies, S.A. (2005). Cyclic nucleotide phosphodiesterases in *Drosophila melanogaster*. Biochem. J. *388*, 333–342.

Dodd, A.N., Gardner, M.J., Hotta, C.T., Hubbard, K.E., Dalchau, N., Love, J., Assie, J.M., Robertson, F.C., Jakobsen, M.K., Goncalves, J., et al. (2007). The *Arabidopsis* circadian clock incorporates a cADPR-based feedback loop. Science *318*, 1789–1792.

Fei, H., Chow, D.M., Chen, A., Romero-Calderon, R., Ong, W.S., Ackerson, L.C., Maidment, N.T., Simpson, J.H., Frye, M.A., and Krantz, D.E. (2010). Mutation of the *Drosophila* vesicular GABA transporter disrupts visual figure detection. J. Exp. Biol. *213*, 1717–1730.

Ferris, J., Ge, H., Liu, L., and Roman, G. (2006). G(o) signaling is required for *Drosophila* associative learning. Nat. Neurosci. *9*, 1036–1040.

Glossop, N.R., Houl, J.H., Zheng, H., Ng, F.S., Dudek, S.M., and Hardin, P.E. (2003). VRILLE feeds back to control circadian transcription of *Clock* in the *Drosophila* circadian oscillator. Neuron *37*, 249–261.

Hamasaka, Y., Rieger, D., Parmentier, M.L., Grau, Y., Helfrich-Forster, C., and Nassel, D.R. (2007). Glutamate and its metabotropic receptor in *Drosophila* clock neuron circuits. J. Comp. Neurol. *505*, 32–45.

Hamasaka, Y., Wegener, C., and Nassel, D.R. (2005). GABA modulates *Drosophila* circadian clock neurons via $GABA_B$ receptors and decreases in calcium. J. Neurobiol. *65*, 225–240.

Harmar, A.J., Arimura, A., Gozes, I., Journot, L., Laburthe, M., Pisegna, J.R., Rawlings, S.R., Robberecht, P., Said, S.I., Sreedharan, S.P., et al. (1998). International Union of Pharmacology. XVIII. Nomenclature of receptors for Vasoactive Intestinal Peptide and Pituitary Adenylate Cyclase-Activating Polypeptide. Pharmacol. Rev. *50*, 265–270.

Harmar, A.J., Marston, H.M., Shen, S., Spratt, C., West, K.M., Sheward, W.J., Morrison, C.F., Dorin, J.R., Piggins, H.D., Reubi, J.C., et al. (2002). The $VPAC_2$ receptor is essential for circadian function in the mouse suprachiasmatic nuclei. Cell *109*, 497–508.

Harrisingh, M.C., Wu, Y., Lnenicka, G.A., and Nitabach, M.N. (2007). Intracellular Ca^{2+} regulates free-running circadian clock oscillation *in vivo*. J. Neurosci. *27*, 12489–12499.

Herzog, E.D., Takahashi, J.S., and Block, G.D. (1998). *Clock* controls circadian period in isolated suprachiasmatic nucleus neurons. Nat. Neurosci. *1*, 708–713.

Hille, B. (2001). Ion channels of excitable membranes, Third Edition (Sunderland, Mass.: Sinauer Associates).

Hyun, S., Lee, Y., Hong, S.T., Bang, S., Paik, D., Kang, J., Shin, J., Lee, J., Jeon, K., Hwang, S., et al. (2005). *Drosophila* GPCR Han is a receptor for the circadian clock neuropeptide PDF. Neuron *48*, 267–278.

Im, S.H., and Taghert, P.H. (2010). PDF receptor expression reveals direct interactions between circadian oscillators in *Drosophila*. J. Comp. Neurol. *518*, 1925–1945.

Jan, L.Y., and Jan, Y.N. (1976). Properties of the larval neuromuscular junction in *Drosophila melanogaster*. J. Physiol. *262*, 189–214.

Kaneko, M., Helfrich-Forster, C., and Hall, J.C. (1997). Spatial and temporal expression of the *period* and *timeless* genes in the developing nervous system of *Drosophila*: Newly identified pacemaker candidates and novel features of clock gene product cycling. J. Neurosci. *17*, 6745–6760.

Katanaev, V.L., Ponzielli, R., Semeriva, M., and Tomlinson, A. (2005). Trimeric G protein-dependent frizzled signaling in *Drosophila*. Cell *120*, 111–122.

Kaupmann, K., Malitschek, B., Schuler, V., Heid, J., Froestl, W., Beck, P., Mosbacher, J., Bischoff, S., Kulik, A., Shigemoto, R., et al. (1998). $GABA_B$-receptor subtypes assemble into functional heteromeric complexes. Nature *396*, 683–687.

Kavanaugh, M.P., Varnum, M.D., Osborne, P.B., Christie, M.J., Busch, A.E., Adelman, J.P., and North, R.A. (1991). Interaction between tetraethylammonium and amino acid residues in the pore of cloned voltage-dependent potassium channels. J. Biol. Chem. *266*, 7583–7587.

Kilman, V.L., Zhang, L., Meissner, R.A., Burg, E., and Allada, R. (2009). Perturbing dynamin reveals potent effects on the *Drosophila* circadian clock. PLoS ONE *4*, e5235.

Kula-Eversole, E., Nagoshi, E., Shang, Y., Rodriguez, J., Allada, R., and Rosbash, M. (2010). Surprising gene expression patterns within and between PDF-containing circadian neurons in *Drosophila*. Proc. Natl. Acad. Sci. USA *107*, 13497–13502.

Lakin-Thomas, P.L., and Brody, S. (1985). Circadian rhythms in *Neurospora crassa*: interactions between clock mutations. Genetics *109*, 49–66.

Lear, B.C., Merrill, C.E., Lin, J.M., Schroeder, A., Zhang, L., and Allada, R. (2005). A G protein-coupled receptor, *groom-of-PDF*, is required for PDF neuron action in circadian behavior. Neuron *48*, 221–227.

Levine, J.D., Casey, C.I., Kalderon, D.D., and Jackson, F.R. (1994). Altered circadian pacemaker functions and cyclic AMP rhythms in the *Drosophila* learning mutant *dunce*. Neuron *13*, 967–974.

Lin, Y., Stormo, G.D., and Taghert, P.H. (2004). The neuropeptide Pigment-Dispersing Factor coordinates pacemaker interactions in the *Drosophila* circadian system. J. Neurosci. *24*, 7951–7957.

Liu, C., Weaver, D.R., Strogatz, S.H., and Reppert, S.M. (1997). Cellular construction of a circadian clock: period determination in the suprachiasmatic nuclei. Cell *91*, 855–860.

Liu, A.C., Welsh, D.K., Ko, C.H., Tran, H.G., Zhang, E.E., Priest, A.A., Buhr, E.D., Singer, O., Meeker, K., Verma, I.M., et al. (2007). Intercellular coupling confers robustness against mutations in the SCN circadian clock network. Cell *129*, 605–616.

Majercak, J., Kalderon, D., and Edery, I. (1997). *Drosophila melanogaster* deficient in Protein Kinase A manifests behavior-specific arrhythmia but normal clock function. Mol. Cell. Biol. *17*, 5915–5922.

Maywood, E.S., Reddy, A.B., Wong, G.K., O'Neill, J.S., O'Brien, J.A., McMahon, D.G., Harmar, A.J., Okamura, H., and Hastings, M.H. (2006). Synchronization and maintenance of timekeeping in suprachiasmatic circadian clock cells by neuropeptidergic signaling. Curr. Biol. *16*, 599–605.

McCormack, T.J. (2003). Comparison of K^+-channel genes within the genomes of *Anopheles gambiae* and *Drosophila melanogaster*. Genome Biol. *4*, R58.

Mehren, J.E., and Griffith, L.C. (2006). Cholinergic neurons mediate CaMKII-dependent enhancement of courtship suppression. Learn. Mem. *13*, 686–689.

Mertens, I., Vandingenen, A., Johnson, E.C., Shafer, O.T., Li, W., Trigg, J.S., De Loof, A., Schoofs, L., and Taghert, P.H. (2005). PDF receptor signaling in *Drosophila* contributes to both circadian and geotactic behaviors. Neuron *48*, 213–219.

Mezler, M., Muller, T., and Raming, K. (2001). Cloning and functional expression of $GABA_B$ receptors from *Drosophila*. Eur. J. Neurosci. *13*, 477–486.

Nagoshi, E., Sugino, K., Kula, E., Okazaki, E., Tachibana, T., Nelson, S., and Rosbash, M. (2010). Dissecting differential gene expression within the circadian neuronal circuit of *Drosophila*. Nat. Neurosci. *13*, 60–68.

Nitabach, M.N., Blau, J., and Holmes, T.C. (2002). Electrical silencing of *Drosophila* pacemaker neurons stops the free-running circadian clock. Cell *109*, 485–495.

Nitabach, M.N., Wu, Y., Sheeba, V., Lemon, W.C., Strumbos, J., Zelensky, P.K., White, B.H., and Holmes, T.C. (2006). Electrical hyperexcitation of lateral ventral pacemaker neurons desynchronizes downstream circadian oscillators in the fly circadian circuit and induces multiple behavioral periods. J. Neurosci. *26*, 479–489.

O'Neill, J.S., Maywood, E.S., Chesham, J.E., Takahashi, J.S., and Hastings, M.H. (2008). cAMP-dependent signaling as a core component of the mammalian circadian pacemaker. Science *320*, 949–953.

Olsen, S.R., and Wilson, R.I. (2008). Lateral presynaptic inhibition mediates gain control in an olfactory circuit. Nature *452*, 956–960.

Parisky, K.M., Agosto, J., Pulver, S.R., Shang, Y., Kuklin, E., Hodge, J.J., Kang, K., Liu, X., Garrity, P.A., Rosbash, M., and Griffith, L.C. (2008). PDF cells are a GABA-responsive wake-promoting component of the *Drosophila* sleep circuit. Neuron *60*, 672–682.

Park, S.K., Sedore, S.A., Cronmiller, C., and Hirsh, J. (2000). Type II cAMP-dependent protein kinase-deficient *Drosophila* are viable but show developmental, circadian, and drug response phenotypes. J. Biol. Chem. *275*, 20588–20596.

Peng, Y., Stoleru, D., Levine, J.D., Hall, J.C., and Rosbash, M. (2003). *Drosophila* free-running rhythms require intercellular communication. PLoS Biol. *1*, E13.

Pollack, I., and Hofbauer, A. (1991). Histamine-like immunoreactivity in the visual system and brain of *Drosophila melanogaster*. Cell Tissue Res. *266*, 391–398.

Reiff, D.F., Ihring, A., Guerrero, G., Isacoff, E.Y., Joesch, M., Nakai, J., and Borst, A. (2005). *In vivo* performance of genetically encoded indicators of neural activity in flies. J. Neurosci. *25*, 4766–4778.

Renn, S.C., Park, J.H., Rosbash, M., Hall, J.C., and Taghert, P.H. (1999). A *pdf* neuropeptide gene mutation and ablation of PDF neurons each cause severe abnormalities of behavioral circadian rhythms in *Drosophila*. Cell *99*, 791–802.

Reppert, S.M., and Weaver, D.R. (2002). Coordination of circadian timing in mammals. Nature *418*, 935–941.

Rothenfluh, A., Abodeely, M., and Young, M.W. (2000). Short-period mutations of *per* affect a *double-time*-dependent step in the *Drosophila* circadian clock. Curr. Biol. *10*, 1399–1402.

Schneider, N.L., and Stengl, M. (2005). Pigment-dispersing factor and GABA synchronize cells of the isolated circadian clock of the cockroach *Leucophaea maderae*. J. Neurosci. *25*, 5138–5147.

Shafer, O.T., Kim, D.J., Dunbar-Yaffe, R., Nikolaev, V.O., Lohse, M.J., and Taghert, P.H. (2008). Widespread receptivity to neuropeptide PDF throughout the neuronal circadian clock network of *Drosophila* revealed by real-time cyclic AMP imaging. Neuron *58*, 223–237.

Sheeba, V., Fogle, K.J., Kaneko, M., Rashid, S., Chou, Y.T., Sharma, V.K., and Holmes, T.C. (2008). Large ventral lateral neurons modulate arousal and sleep in *Drosophila*. Curr. Biol. *18*, 1537–1545.

Shortridge, R.D., Yoon, J., Lending, C.R., Bloomquist, B.T., Perdew, M.H., and Pak, W.L. (1991). A *Drosophila* phospholipase C gene that is expressed in the central nervous system. J. Biol. Chem. *266*, 12474–12480.

Stanewsky, R., Jamison, C.F., Plautz, J.D., Kay, S.A., and Hall, J.C. (1997). Multiple circadian-regulated elements contribute to cycling *period* gene expression in *Drosophila*. EMBO J. *16*, 5006–5018.

Stoleru, D., Peng, Y., Nawathean, P., and Rosbash, M. (2005). A resetting signal between *Drosophila* pacemakers synchronizes morning and evening activity. Nature *438*, 238–242.

Ueno, K., Kohatsu, S., Clay, C., Forte, M., Isono, K., and Kidokoro, Y. (2006). Gsα is involved in sugar perception in *Drosophila melanogaster*. J. Neurosci. *26*, 6143–6152.

Wegener, C., Hamasaka, Y., and Nassel, D.R. (2004). Acetylcholine increases intracellular Ca^{2+} via nicotinic receptors in cultured PDF-containing clock neurons of *Drosophila*. J. Neurophysiol. *91*, 912–923.

Welsh, D.K., Logothetis, D.E., Meister, M., and Reppert, S.M. (1995). Individual neurons dissociated from rat suprachiasmatic nucleus express independently phased circadian firing rhythms. Neuron *14*, 697–706.

Wolfgang, W.J., Roberts, I.J., Quan, F., O'Kane, C., and Forte, M. (1996). Activation of protein kinase A-independent pathways by $G_s\alpha$ in *Drosophila*. Proc. Natl. Acad. Sci. USA *93*, 14542–14547.

Yasuyama, K., and Meinertzhagen, I.A. (1999). Extraretinal photoreceptors at the compound eye's posterior margin in *Drosophila melanogaster*. J. Comp. Neurol. *412*, 193–202.

Yoshii, T., Wulbeck, C., Sehadova, H., Veleri, S., Bichler, D., Stanewsky, R., and Helfrich-Forster, C. (2009). The neuropeptide Pigment-Dispersing Factor adjusts period and phase of *Drosophila*'s clock. J. Neurosci. *29*, 2597–2610.

Yuan, Q., Lin, F., Zheng, X., and Sehgal, A. (2005). Serotonin modulates circadian entrainment in *Drosophila*. Neuron *47*, 115–127.